FINAL REPORT

THE TERF PROGRAM AND ITS APPLICATIONS TO THE CALCULATION OF FALLOUT RADIATION DOSE

January, 1969

Office of Civil Defense
Work Unit 3123A
Contract No. N0022867C2341

Mathematical Applications Group, Inc.
180 S. Broadway
White Plains, New York

NRDL-TRC-68-56

77

FINAL REPORT

THE TERF PROGRAM AND ITS APPLICATIONS TO THE CALCULATION OF FALLOUT RADIATION DOSE

R. Goldstein

January, 1969

Sponsored by the Office of Civil Defense, Office of the Secretary of the Army through the Technical Management Office, U. S. Naval Radiological Defense Laboratory.

OCD Work Unit 312A

Contract No. N0022867C2341

Mathematical Applications Group, Inc.
180 S. Broadway
White Plains, New York

NRDL-TRC-68-56

ACKNOWLEDGEMENTS

It is a pleasure to acknowledge the advice and technical cooperation provided during the course of this study by Drs. E. Corry of USNRDL and D. Bensen of OCD. This work was also materially aided by the many helpful technical discussions with Dr. M. Kalos and the programming expertise of Mr. R. Nagel who was responsible for implementing the FRET program.

ABSTRACT

TERF is a Monte Carlo radiation transport code for computing γ-ray dose due to fallout on non-uniform terrain. The code as developed in this study incorporates extensive geometry capabilities including the unique ability to convert elevation contour line data into three-dimensional terrain representations. A variety of calculations concerned with the effects on the dose of various terrain features, structures and vegetation, are described.

TABLE OF CONTENTS

TABLE OF CONTENTS (Continued)

TABLES

FIGURES

1. INTRODUCTION

In the past, calculations of ground level radiation doses due to nuclear weapon fallout have been restricted to problems involving rather simple representations of the terrain. Generally, the ground has been treated as a uniform plane with the radiation source distributed over the surface. This simplified treatment does not permit a realistic assessment of the shielding effects of common terrain features.

For this reason, MAGI, in conjunction with USNRDL, initiated a study program directed toward the development of a computer program capable of performing radiation transport calculations on non-uniform terrain. The ultimate goal of this study was to develop and demonstrate a code which could

a) faithfully represent the geometry of large areas of the ground,

b) permit the representation of non-terrain features such as houses, forests, etc.,

c) provide the user with a simple means for describing the terrain,

d) compute the fallout radiation dose at one or more specified points.

The computer program TERF, discussed in the remainder of this report, satisfies all of the above requirements and is currently operational on the CDC 6600. Section 2 discusses

the basic concepts employed in the program, briefly summarizes its capabilities and describes qualitatively the types of calculations which were done. Section 3 provides a more detailed description of the code and its applications. Finally, Section 4 gives the results of calculations which both demonstrate the capabilities of the code and provide useful data for weapons effects analysts.

A brief description of the FRET program, developed during the latter stages of this study, is given in Appendix B. This code incorporates the geometry capabilities of TERF but solves the gamma ray adjoint or "backward" problem (hence the name FRET).

2. SUMMARY

2.1 Brief Description of TERF

TERF (TERrain Features Code) is based to a large extent on the SAM-C program[1] developed by MAGI for the Army Ballistic Research Laboratory. The two programs are, in fact, almost identical except for additional routines in TERF which permit the treatment of complex terrain geometry and fallout radiation sources. Basically, TERF is a Monte Carlo program written in FORTRAN, which calculates the time dependent transport of neutrons* or gamma rays through matter. It is composed of a series of independent routines which perform the following functions:

1. process cross-section data,
2. process geometry data,
3. perform the transport calculation,
4. edit the results.

The program requires as input a specification of the geometry, the elemental composition of each geometric region, and a specification of the position-energy-time-angular distribution of the radiation source. The program selects individual particles (or histories) from the given source

* The ability to perform neutron calculations is a remnant from the SAM-C code and is not particularly useful for fallout problems. However, this capability could ultimately be used for certain weapons effects calculations, such as a point neutron source in air over non-uniform terrain.

distribution and tracks them through a series of interactions within the geometry until such time as the particle history is terminated. The tracking of a particle can be terminated for any of the following reasons.

1. The particle energy falls below a specified "cutoff energy".
2. The elapsed time spent by the particle in traversing the geometry exceeds a specified "cutoff time".
3. The particle escapes from the geometry by crossing an external boundary.
4. The importance of the particle (its expected contribution to the dose) becomes insignificant.

For each geometric region traversed by a given particle, the code computes the flux per unit time per unit energy as a function of time and energy. The flux contribution for a given particle is defined as its total path length contribution in a region divided by the volume of the region. Individual particle flux contributions are accumulated so that the end result of the tracking process is the total flux in each region in a specified group of energy and time bins. At the user's option, the problem can also be made time independent. The code has the additional capability of being able to compute fluxes at specified points within the geometry, as well as in finite regions.

Both SAM-C and TERF make use of the Combinatorial Geometry method, a powerful technique for representing three dimensional geometry in a computer. This method is described more fully in Section 3. In brief, it enables the user to represent complicated three dimensional geometric shapes by combining certain basic figures (i.e., spheres, cylinders, boxes, ellipses, cones, etc.).

In theory, Combinatorial Geometry as it exists in SAM-C, could be used to represent non-uniform terrain by "mocking up" every hill and valley in terms of one or more of the allowed basic figures. In practice, however, the input preparation time as well as demands on computer memory for any realistic area of terrain would be prohibitive. Therefore, TERF was given the additional capability to accept a simple description of the terrain and, by internal processing, convert that input to the Combinatorial Geometry format required by the remainder of the code.

2.2 Terrain Representation

The code employs what is probably the simplest method of representing complex areas of the ground. That is, the terrain input consists of a series of elevation contour lines of essentially any degree of complexity and covering any desired surface area. Each contour line is described by its altitude Z and a set of points in the X-Y (horizontal) plane which define the contour line boundary. The code processes this contour line input, constructing a three

dimensional mock-up of the ground in terms of basic geometric figures. In addition to contour line data, the code will also accept descriptions of non-terrain features, such as houses and wooded areas. These features may be located anywhere on, above or below the surface of the ground. The calculational methods employed in this input processing routine are described in Section 3.

2.3 Representation of Fallout Fields

A new source picking routine was devised to enable the radiation source to be deposited over the ground in much the same manner as nuclear weapon fallout. That is, the area of the fallout field is specified and individual source particles are deposited uniformly within this area according to the following rules.

1. Particles deposited on the ground are placed on the surface of the ground.
2. Particles deposited on any other solid object are placed on the top surface of that object (i.e., the roof of a house).
3. Particles falling on a wooded region are distributed within that region according to any given input distribution.

The initial energy spectrum (and time distribution, if desired) of the source are completely arbitrary.

In summary, then, the TERF program provides a powerful

method for both accurately representing non-uniform terrain and computing the radiation environment at any desired location.

Many of the capabilities described above have been demonstrated via a rather large variety of calculations. These problems were designed not only to test the code but to provide information on the effects of various terrain types, structures and vegetation. Terrain variations included simple hills and valleys, ravines, and rolling hills. Structures ranged from simple box-shaped houses to a detailed description of a complete housing development. Areas of vegetation such as typical forests and crop fields were also investigated. The effects of these features were, in many cases, quite striking, indicating the practical necessity of employing both accurate and detailed methods for their solutions.

3. DESCRIPTION OF THE TERF PROGRAM

TERF is composed of two main programs, TERRA and FIRMA. Program TERRA is basically an input handling routine which reads in the geometry input as well as data for cross sections, source distribution, material compositions, and output edit specifications. This input is processed into a form required by program FIRMA which performs the Monte Carlo calculation and edits the results.

Since this project was primarily concerned with incorporating new geometry capabilities into the code, this section will be mainly confined to a description of the geometry handling routines in program TERRA. A complete description of the remainder of the program is found in Reference 1. The geometry capabilities of the code may, for purposes of discussion, be conveniently divided into the following three topics.

1. Combinatorial Geometry
2. Representation of terrain
3. Representation of non-terrain features

These are discussed separately below along with a description of how the program simulates fallout radiation fields.

3.1 Combinatorial Geometry

In order to perform Monte Carlo studies of radiation transport in three dimensions, one must first prepare a

mathematical model of the geometry of the problem. The Combinatorial Geometry technique was developed to permit an accurate yet relatively straightforward construction of such a model.

In effect, the geometric description subdivides the problem space into unique regions. Each region is the result of combining one or more of the following geometric bodies.

1. Rectangular Parallelepiped (RPP)
2. Box (an RPP randomly oriented in space)
3. Sphere
4. Right Circular Cylinder
5. Right Elliptic Cylinder
6. Truncated Right Angle Cone
7. Ellipsoid
8. Right Angle Wedge
9. Arbitrary Convex Polyhedron of 4,5, or 6 sides

The basic technique for the description of the geometry consists of defining the location and shape of the various physical regions in terms of the intersections and unions of the volumes contained in the above set of simple bodies. A special operator notation involving the symbols (+), (-), and (OR) is used to describe the intersections and unions. These symbols are used by the program to construct tables used in the particle tracking portion of the problem.

If a body appears in a region description with a (+)

operator, it means that the region being described is wholly contained in the body.

If a body appears in a region description with a (-) operator, it means that the region being described is wholly outside the body.

If the body appears with an (OR) operator, it means that the region being described includes all points in the body. In some instances, a region may be described in terms of subregions lumped together by (OR) statements.

The technique of describing a physical region is best illustrated by an example. Consider an object composed of a sphere into which is inserted a cylinder. This is shown in cross section in Figure 3.1(a).

To describe the object, we take a spherical body penetrated by a cylindrical body (Figure 3.1(b)). Each body is numbered. Consider the sphere as body No. 1 and the cylinder as body No. 2. If the materials in the sphere and cylinder are the same, then they can be considered as one physical region, say region 100 (Figure 3.1(c)).

The description of region 100 would be:

100 = (OR 1) (OR 2).

This means that a point is in region 100 if it is <u>either</u> inside body 1 <u>or</u> inside body 2.

If different materials are used in the sphere and cylinder, then the sphere with a cylindrical hole in it would be given a different region number (say 200) from

that of the cylinder (300).

The description of region 200 would be (Figure 3.1(d)):

200 = (+1) (-2).

This means that points in region 200 are all those points inside body 1 which are not inside body 2.

The description of region 300 is simple (Figure 3.1(e)):

300 = (+2).

That is, all points in region 300 lie inside body 2.

This technique, of course, can be applied to combinations of more than two bodies and such region descriptions could conceivably contain a long string of (+), (-) and (OR) operators. The important thing to remember is that every spatial point in the geometry must be located in one and only one region.

Basically, then, Combinatorial Geometry permits one to represent any three dimensional object which can be broken down into component parts, where each component is one of the nine bodies listed above.

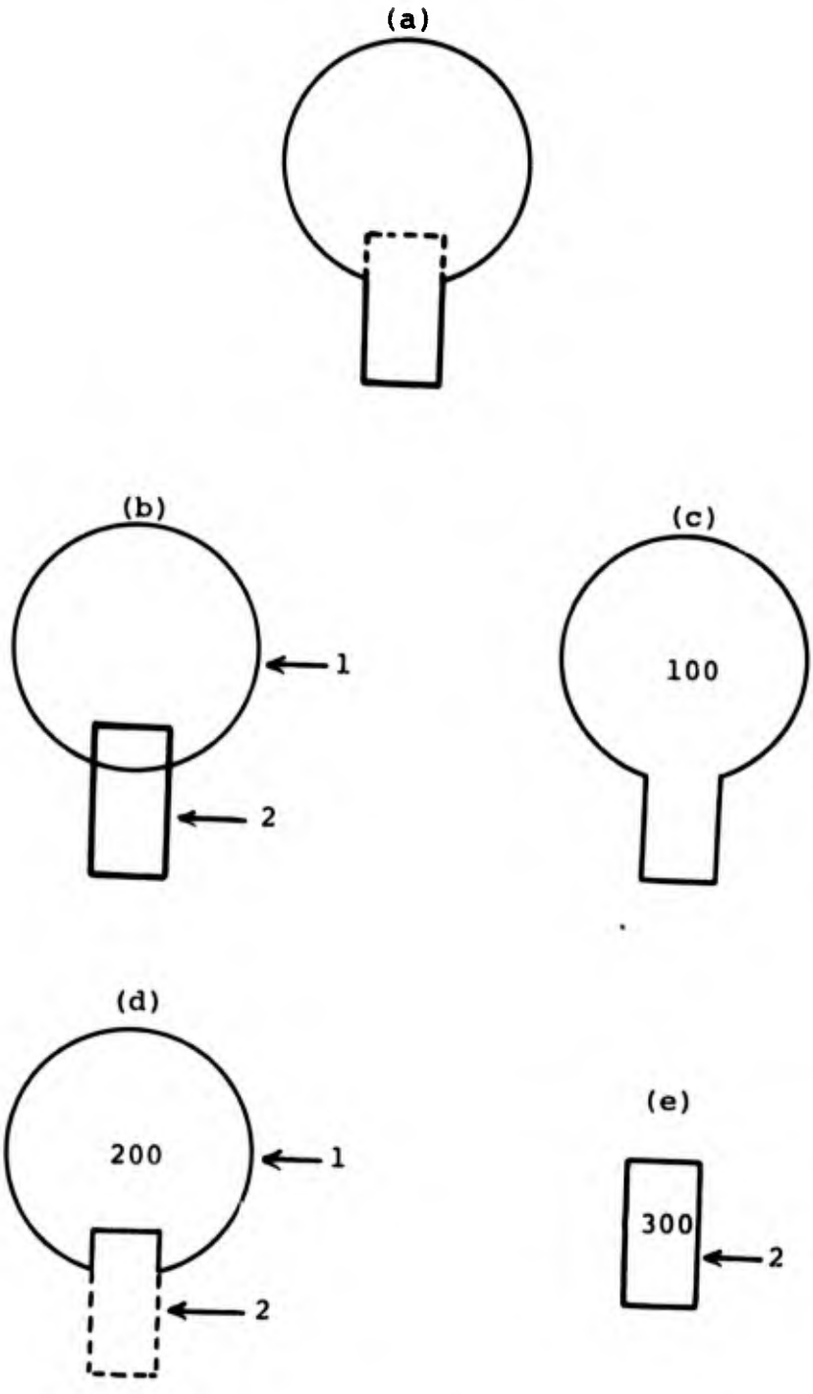

Figure 3.1 - Examples of Combinatorial Geometry Method

3.2 Terrain Simulation Method

The most efficient means of adding terrain handling capabilities to the program was to represent the ground within the overall framework of the Combinatorial Geometry technique. That is, the terrain would be built up from basic bodies in the same manner as any other geometric region in the problem. To accomplish this, a new body type was devised. Namely, a 7-sided polyhedron having the following properties. A horizontal rectangular base, 4 vertical sides, and a top composed of 2 triangular surfaces having a common boundary. Two views of this body are shown in Figure 3.2.

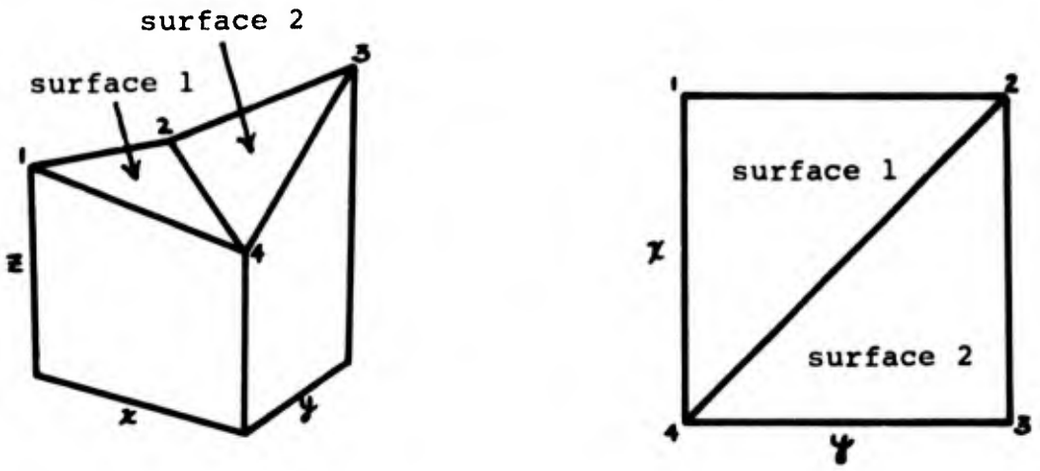

orthogonal top

Figure 3.2 - Basic Body Used To Represent Terrain

These bodies, when placed adjacent to one another could then be used to represent the undulations of the terrain surface.

For example, Figure 3.3 shows a vertical slice taken through an array of these bodies.

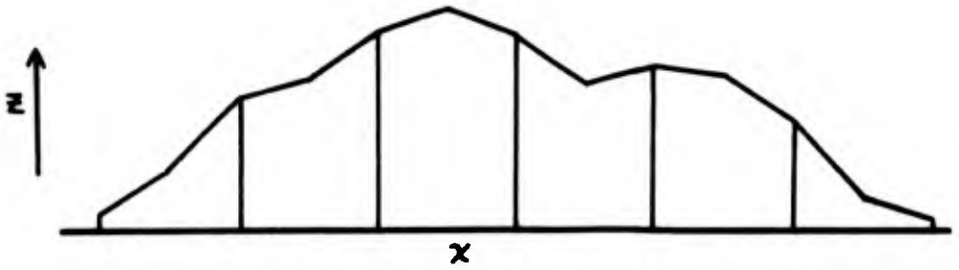

Figure 3.3 - Profile of Terrain Formed by Polyhedra

It is apparent that the slopes of the two upper triangular faces are determined by the Z coordinates of the four upper corners of the body. These, in turn, are determined by the height of the terrain at these four corners. The problem, then, is to determine the altitude of the ground at the four top corners of every polyhedron. This is done in the following manner.

A two dimensional horizontal grid is specified on input. Each cell within this grid will contain a 7-sided polyhedron. One or more elevation contour lines are then described, with each line defined by an altitude Z and a set of (X,Y) points relative to the origin of the grid. Figure 3.4 is an example of a grid, two contour lines, and a set of points for each contour. Note that the grid boundaries are assumed to form an external rectangular contour line at sea level altitude.

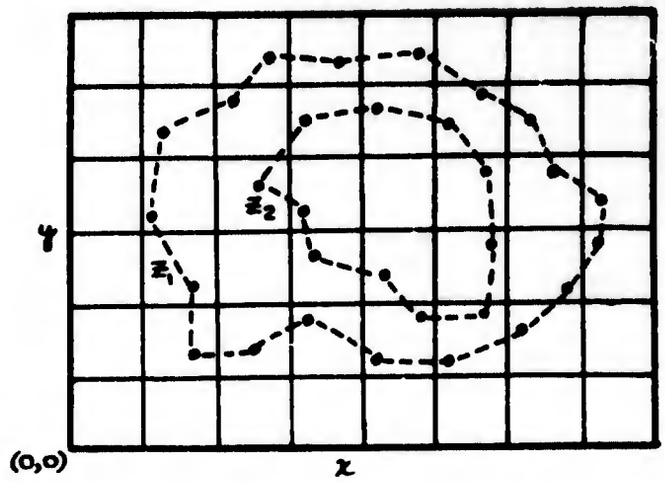

Figure 3.4 - Example of Grid and Terrain Contours

This is all the input needed to describe the terrain. The program uses the given contour points to compute the altitude of the ground at every intersection of the X and Y grid lines (lines perpendicular to the X and Y axes). Thus, the Z coordinate of each of the four corners of every grid cell is defined. A 7-sided polyhedron is then "placed" in every grid cell with the four Z coordinates determining the orientation of the two upper faces. What we have, then, is an array of triangular surfaces which are pieced together to follow the surface contour of the ground.

The calculation of the altitudes at each grid cell corner is relatively straightforward and is based on a linear interpolation between contour lines. For each contour line the code assumes that straight line segments may be drawn connecting the given (X,Y) points. Thus, small irregularities in a contour line may be preserved only by giving a sufficient number of points on its perimeter. Each of these straight line segments is then examined for an intersection

with one or more of the X and Y grid lines. These intersection points are stored along with their corresponding altitudes. After all contour lines have been treated in this manner, the original set of input data points are of no further use. The code has essentially reconstructed a new set of points, each of which lies on an X or Y grid line. It is apparent from this that the fineness of the grid mesh is at least as important as the number of contour points in preserving the "lay of the land". For example, if two consecutive points on the same contour line lie within the same grid cell, the line joining the two will not cross any grid lines and no intersection will be found. This tends to "wash out" any fine structure in the contours. This situation can be avoided by decreasing the size of the grid cells, while increasing the number of cells, so that two consecutive points lie in adjacent cells rather than in the same cell.

Once all intersections are recorded, the altitudes at the corners of each grid cell are calculated using a four-point interpolation. The code scans all of the intersection points along the two grid lines passing through a given corner and selects the closest point in the positive x direction, the closest in the positive y direction, and the closest in the negative x and negative y directions. Denoting each of these intersection points by an integer 1 to 4, the code

computes the altitude, Z, at the grid cell corner from the following equation.

$$Z = \frac{\sum_{n=1}^{4} Z_n/R_n}{\sum_{n=1}^{4} 1/R_n}$$

where z_n is the altitude of the ground at the Nth intersection and R_n is the distance between the grid cell corner and the Nth intersection point. This equation weights the altitude at each intersection by its distance from the grid cell corner, so that as the corner approaches the intersection, its altitude will approach that at the intersection. The above procedure is repeated for each corner in the grid.

Thus, having started with a set of digitized contour line data, the code has computed the altitude of the ground at a systematic set of points defined by the grid mesh. As mentioned earlier, these altitudes determine the slope of the ground in each cell within the grid.

It should also be noted that the geometry of the problem need not be entirely enclosed in the grid. The grid merely defines one area of the geometry, within which the terrain may assume any given non-uniformity. That is, all contour lines must be completely contained within the grid boundaries. Outside the grid, however, the ground is assumed to be flat, extending an arbitrary distance in all directions.

3.3 Representing Non-Terrain Features

Objects which are not part of the general terrain may also be included in any problem. These are of two distinct classifications. Those that lie outside the grid (in the area of flat ground) are described in the normal Combinatorial Geometry format. Thus, any object describable by this technique can be located anywhere outside the grid. These could include houses, vehicles, people, etc.

Within the grid area, the user has the option of employing a slightly modified Combinatorial Geometry format. In general, the altitude of the ground at any given point in the grid is not precisely known to the user. Thus, the required X,Y,Z coordinates of a geometric body cannot be completely specified. To circumvent this, the code permits the Z coordinate of any body to be specified relative to the ground. That is, a coordinate may be given as X,Y,ΔZ, where ΔZ is a distance above or below ground. The code determines the altitude of the ground at point (X,Y) and locates the body a distance ΔZ from that altitude level.

Finally, the code provides a simple method of representing certain non-terrain features which are repetitive. Under this option, the geometry specifications for an object which appears many times at different locations need not be repeated for each location. The allowed non-terrain features are restricted to two types, called "structures". The properties of the two allowed structures are discussed

below.

Structure Type 1

This structure was devised to allow the easy representation of simple box-shaped houses or objects of similar shape. The structure is defined by an outer box whose four walls are vertical and whose top and bottom surfaces are parallel to the x, y plane. The bottom surface, or "floor" may be located any desired distance below the ground surface. This outer box may, in turn, contain other boxes, spheres, or right circular cylinders. As an example, a simple multi-room house could be represented with a spherical or cylindrical "man model" in each room. This is shown in Figure 3.5. The internal boxes would contain air, while the shaded portion of the outer box could be any structural material such as concrete.

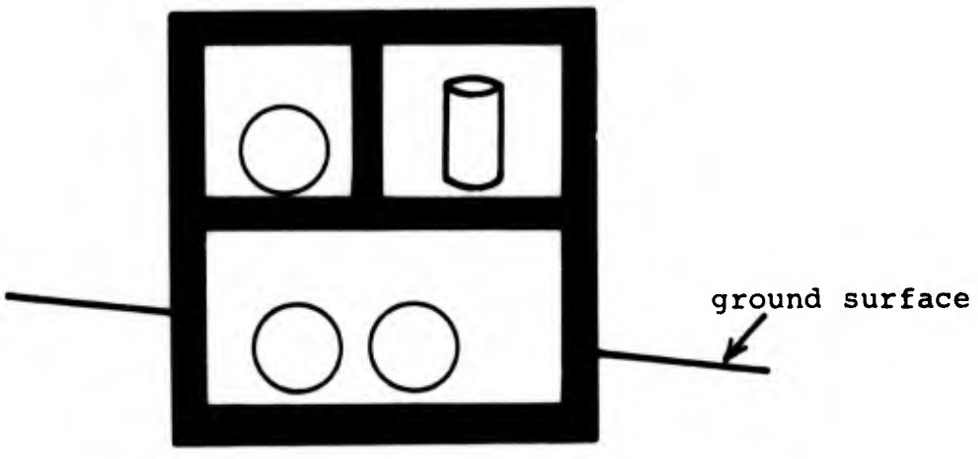

Figure 3.5 - Example of Structure Type 1

A structure, once defined, may be located at any number of sites within the grid merely by specifying a set of locations for the outer box. The internal bodies are automatically moved to their proper positions at each of these locations. Furthermore, any number of different structures can be defined so that the terrain can be dotted with houses of various sizes. The only restriction on the location of a structure is that it be wholly contained within a grid cell.

Structure Type 2

The second allowed structure was devised primarily for the representation of irregularly shaped wooded areas. This structure is also a six sided body, with four vertical sides. The top and bottom surfaces, however, are parallel to the surface of the ground rather than parallel to the x-y plane as in the case of type 1. The only restriction on the orientation of the vertical sides is that they form a convex set (the angle between any two adjacent sides must be less than 180°). The outer polyhedron may, in turn, contain other polyhedrons, again having vertical sides and top and bottom surfaces parallel to the ground. An example is shown in Figure 3.6.

Structure type 2 would generally be used to describe wooded areas by assigning to it a homogeneous chemical composition representative of such an area (a low density mixture of wood and foliage, for example). Internal poly-

hedrons containing air might also be inserted to represent clearings in the forest. Once a given structure has been defined it may be located in as many different grid cells as desired, with the restriction that it be completely contained within either triangular half of a grid cell. The reason for this is that the bottom surface of the structure must be parallel to the ground and the slope of the ground is only constant within one of the triangular sections of a cell.

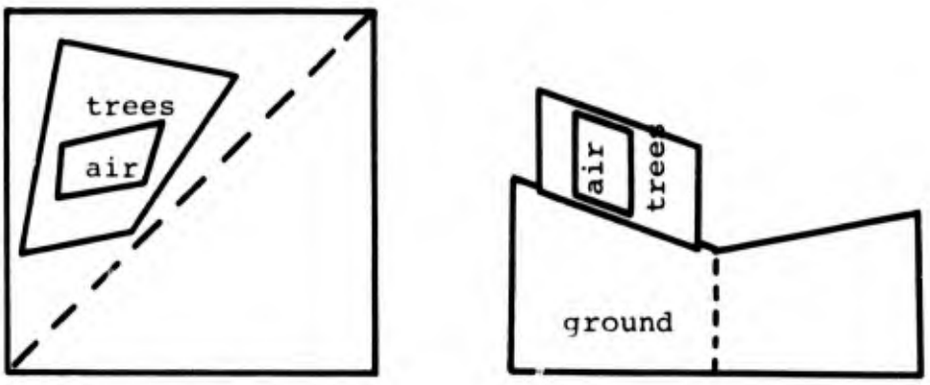

Figure 3.6 - Example of Structure Type 2

3.4 Simulation of Fallout Patterns

A special source routine was written to simulate the distribution of fallout radiation sources. A rectangular area, within which the sources are to be deposited, is specified on input and assumed to be (a) parallel to the x-y plane and (b) located above the highest body in the geometry. This rectangle may be located anywhere in the geometry and need not be within the confines of the grid. Source particle locations (x,y coordinates) are picked at random within this rectangular area. A second rectangle, smaller than the first, may also be specified. In this case, source points are picked within the outer rectangle but not within the inner one. Thus, it is possible to investigate the contributions of fallout on different areas of the terrain. For example, a rectangular area over the roof of a house may be "cut out" and the dose will be computed as if no fallout had been deposited on the roof. Then, in a second problem, the source rectangle may be made to cover only the roof, giving a separate determination of the roof-top contribution. It might be mentioned at this point that, although the present version of TERF is restricted to rectangular source patterns, it is a trivial job to extend the code to cover almost any desired shape.

At any rate, once the x-y coordinates of a source point have been picked, the particle is "dropped" directly downward until the first non-air region is encountered.

The chemical composition of that region is then investigated for the following three possibilities.

1. The region is neither vegetation nor water. In this case the source point is placed on the upper surface of that region. Thus, sources will be located on the top surface of the ground, buildings, etc.
2. The region has been designated as containing vegetation (i.e., forest, crops, etc.). If such a region exists in the problem, the distribution of sources in this region must be supplied on input. This distribution gives the fraction of source particles to be deposited as a function of depth from the top of the region. For example, a forest region may have a total depth of 30 ft. with 0.3 of the particles falling on the forest to be located in the upper 10 ft. and 0.2 in the lower 20 ft. When a particle hits the top of this region, a random number n is picked between 0 and 1. For $n \leq .3$, the particle is placed at random between 0 and 10 ft. from the top surface. For $.3 < n \leq .5$, it is located at random from 10 to 30 ft. from the top. For $n > .5$, the particle is allowed to drop completely through the forest and continues falling until the next non-air region is reached.

3. The region has been designated as water. If a body of water exists in the problem the fraction of fallout particles soluble in water must be given as input. This soluble fraction will be located at random within the water, while the remainder will be allowed to settle to the bottom.

3.5 Other Features of TERF

As mentioned earlier, this section was primarily devoted to a discussion of those segments of TERF which differ from the SAM-C code. Still, it would not be complete without at least a brief description of some of the other important features of the code.

3.5.1 Input and Output Energy Spectra

The source spectrum is completely arbitrary, so long as the energy range lies within the range of cross sections available to the code. For gamma rays, these cross sections extend from .01 Mev up to 10 Mev and include Compton scattering, pair production and photoelectric absorption. Input consists of the integral spectrum between upper and lower source energies (i.e., fraction of gammas emitted above E vs. E).

Output energies are specified as a discrete set of energy bins, within which the flux is to be edited. These

bins, of arbitrary number and size, must extend from the lower or cutoff energy to the upper energy of the problem. The cutoff energy may, of course, be below the lower energy of the source. The output edit will provide the flux in each of these energy bins for every desired geometric region. In addition, the energy integrated flux is given.

3.5.2 Point Detectors

Particle fluxes in the above energy bins may be obtained at specified points as well as in regions of finite volume. The input need specify only the number of such points and their X,Y,Z coordinates. While there is no limit to the number of points, each requires a considerable amount of additional computing. A rough rule of thumb is that if a given problem can be run in time T with no point detectors, the same problem with n detectors will run (n+1)xT. Thus, in those cases where flux in a finite volume will suffice, point detectors should be avoided.

3.5.3 Importance Sampling

Importance sampling is a method of biasing the problem so that most of the computing time is spent tracking those particles which can contribute significantly to the flux or dose. TERF incorporates three methods to achieve this.

1. Region dependent biasing, where geometric regions are assigned an importance determined by their location relative to the regions or points where answers are desired.
2. Angular dependent biasing, whereby particles traveling in the "right" directions (toward the regions or points of interest) are accentuated while those traveling in the "wrong" direction are relatively neglected.
3. Energy dependent biasing, where particles having certain energies are enhanced more than others.

While the use of importance sampling in TERF is a lengthy subject, suffice it to say that the proper employment of these techniques can vastly improve the computing efficiency of the code for any given problem.

3.5.4 Dose Computation

The basic quantity calculated by TERF is the flux (γ/cm^2 per source γ) in a discrete set of output energy bins. Flux is converted to an energy integrated dose via the following equation.

$$DOSE = \sum_{E} \phi(E) R(E) \text{ where}$$

$\phi(E)$ = flux in energy bin E

$R(E)$ = average flux-to-dose conversion factor (dose per unit flux) in energy bin E.

From the form of the above equation it is obvious that R(E) need not be a dose conversion factor but can be any desired flux dependent quantity, such as the gamma ray heating cross section.

3.5.5 Time Dependence

TERF enables the user to compute particle fluxes as a function of time as well as energy and position. The user may select any desired time bin structure for the problem. Output fluxes will be given in this bin structure in the edit. A time-cutoff must also be specified, which instructs the code to cease tracking all particles which have "aged" beyond this cutoff. During the tracking process the code computes the flight time of a particle between collision points from the velocity of light (or particle energy for neutrons). Interactions are assumed to occur instantaneously. By accumulating the flight times for each particle, the code is capable of storing particle fluxes in the proper output time bin. Time dependent sources may also be treated by supplying a table of time values and the integrated source up to each time.

3.5.6 Variance Estimates

The output edit of TERF also supplies the "coefficients of variation" for the problem. These coefficients (equal to the standard deviation of the flux divided by the flux)

are given in terms of percent and are indicative of the percentage errors in the computed results. To obtain these coefficients, the code subdivides the problem into statistical groups of source particles. The average flux for each group is obtained by averaging the individual flux contributions of each particle in the group. Once obtained, these group averaged fluxes are used to compute the variance from the following equation.

$$C = \frac{\sqrt{\sum_n \phi_n^2 - G \cdot \left(\sum_n \phi_n\right)^2}}{(1-G) \cdot \sum_n \phi_n} \cdot 100$$

Where

C = coefficient of variation in percent

ϕ_n = average flux in the n^{th} statistical group

G = number of particles per group divided by the total number of particles treated in the problem.

3.6 TERF Flowchart

Figure 3.7 is a macroscopic flowchart of the TERF program showing the basic flow of the calculation. The chart also indicates the functions of the major subroutines in the program.

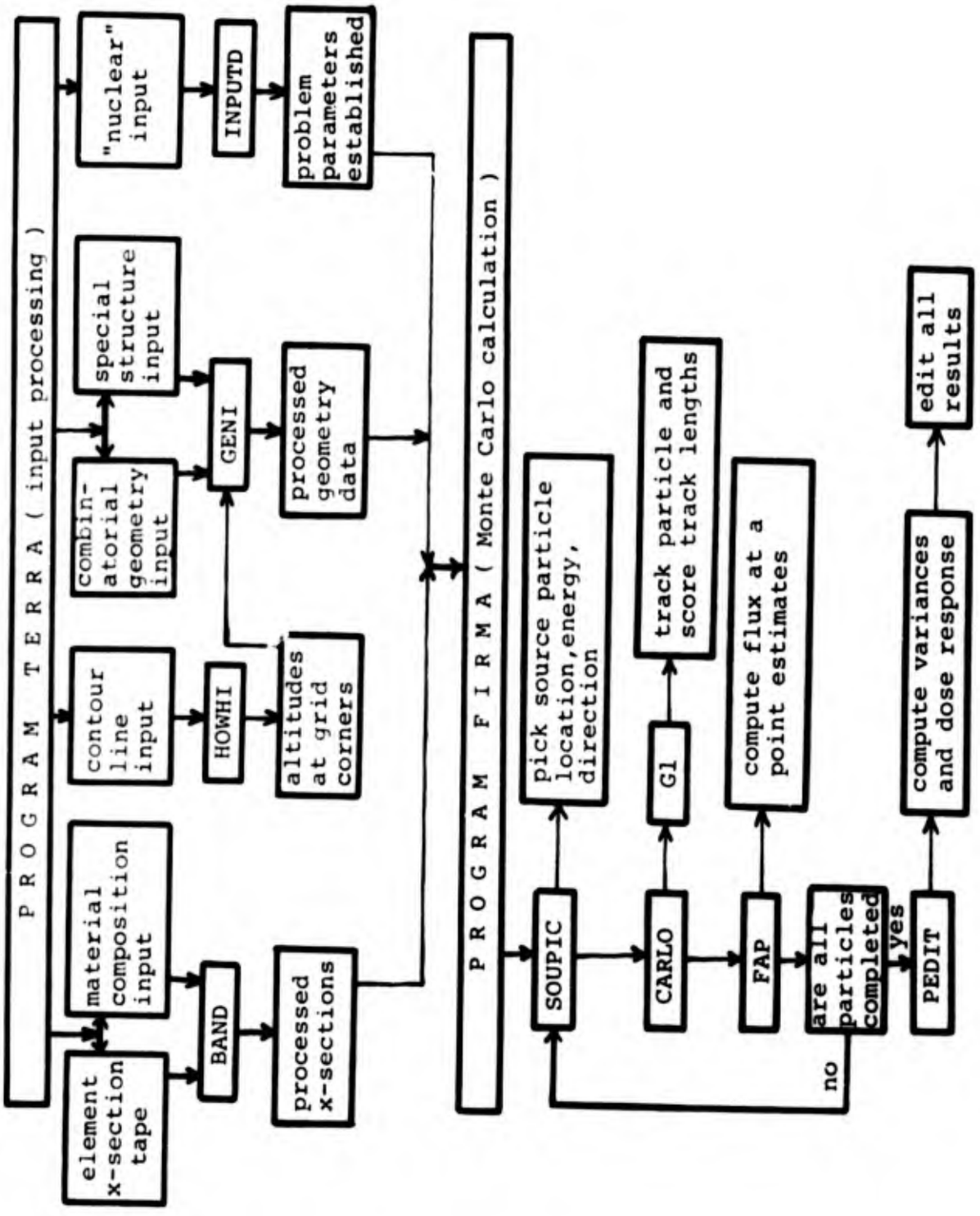

Figure 3.7 - Macroscopic TERF Flowchart

4. Applications of TERF

A wide variety of calculations were performed using the TERF program. As mentioned earlier, these calculations were, to a large extent, intended to demonstrate the capabilities of the code, rather than to provide a systematic study of terrain effects. Thus, the scope of these problems covers a rather broad range of terrain effects without providing an exhaustive parametric study of any one effect. For this reason, it is impractical to attempt any detailed discussion of the calculated results and the remainder of this section will be limited, for the most part, to a description of each problem and its numerical results.

4.1 General Input Parameters

The following input quantities were constant for all problems.

Source Energy

The fallout radiation source was represented by a Co^{60} spectrum. Thus, half the gammas were emitted at 1.17 Mev and the other half at 1.33 Mev.

Dose Conversion Factors

As explained in Section 3.5.4, a set of flux-to-dose conversion factors R(E) is required to convert the calculated fluxes to integrated dose.

Fluxes were computed in 7 energy bins covering the

range .03 Mev to 1.33 Mev. Table 4.1 gives the limits of these bins and the dose conversion factors R(E) in each bin. R(E) was computed on the basis of 1 Roentgen being equivalent to 87.7 ergs/gm of absorbed energy in air[2].

Table 4.1 - Flux-to-Dose Conversion Factors

Energy E (Mev)	R(E) - mR/hr/γ/cm^2-Sec.
1.33 - 1.15	.00213
1.15 - .95	.00178
.95 - .75	.00149
.75 - .55	.00117
.55 - .35	.00078
.35 - .10	.00032
.10 - .03	.00013

The results of all problems are given in units of $\frac{\text{mR/hr}}{\text{curie/Ft}^2}$. These units are obtained by multiplying the quantity $\Sigma\phi(E)R(E)$ by the product G_oxA, where G_o is the emission rate of 1 curie of C_o^{60} ($7.4\text{x}10^{10}$ γ/sec) and A is the source area in ft^2.

Material Compositions

The compositions used for air and ground are given in Table 4.2.

Table 4.2 - Compositions of Air and Ground

Material	Spec. Gravity	Element	Weight Fraction
Air	.00122	N	.78
		O	.22
Ground	2.04	H	.01
		O	.51
		S_i	.35
		K	.13

Compositions other than the above are defined in the descriptions of the individual problems.

4.2 Accuracy and Computer Times

Based on calculated deviations, the total doses in these problems are, in general, accurate to about 10%. While this does not represent extraordinarily good accuracy, it must be remembered that the primary purpose of these calculations was to test the capabilities of the code. Thus, rather than concentrating the available machine time on a few problems, the philosophy of the calculational effort was to run as large a variety of problems as possible.

Running time, on a CDC 6600 computer, varied from about 5 minutes for problems containing relatively simple geometries up to about 30 minutes for the more complex configurations.

4.3 Problem Descriptions and Results

The calculations performed with TERF can be conveniently divided into the following three categories.

a) Effects of terrain features

b) Effects of vegetation

c) Effects of structures

Each of these categories is treated below in a separate section.

4.3.1 Effects of Terrain Features

4.3.1.1 Hills and Valleys

The initial set of TERF calculations involved five problems containing the following relatively simple terrain features.

1. flat ground
2. 100 ft. hill
3. 1000 ft. hill
4. 100 ft. valley
5. 1000 ft. valley

The geometry input to each of these problems consisted of a set of six contour lines in the form of concentric circles. The (x,y) points describing each contour were the same for all problems and only the altitudes z were varied from problem to problem. A general definition of each contour line is given in the following table, where Zmax represents the altitude of the inner contour line (Zmax is posi-

tive for a hill and negative for a valley).

Contour Line	Diameter(Meters)	Altitude (fraction of Zmax)
1	270	.2
2	220	.4
3	170	.6
4	110	.8
5	70	.9
6	20	1.0

The height of the inner contour line is given below for each problem.

Problem	Zmax(Meters)
1	0.0
2	30.5
3	305.0
4	-30.5
5	-305.0

The grid containing these contours was a 300 meter square, divided into a 12x12 mesh and having zero altitude at the outer boundary. The overall diameter of the hills and valleys was,therefore, about 1000 ft. It should be noted that the area inside the inner contour is not flat in these problems (except for Prob. 1) due to the relative locations of contour points and grid lines. This area is actually slightly "rounded" reaching a peak at Zmax in the center of

the contour. The ground region outside the grid was flat and the total area in the problems covered a distance of about 6 mean free paths. This area accounts for more than 98% of the dose at the detector point. In each problem a dose detector point was located 3 feet above the surface of the ground at the center of the inner contour. The fallout source was deposited uniformly over the entire surface of the ground.

The results are shown in Fig. 4.1, where relative dose is plotted as a function of the altitude of the ground below the detector. The flat ground case, being a standard for comparison, is assigned a relative dose of 1.0. The absolute dose for this case is $4.76 \times 10^5 \frac{mR/hr}{curie/ft^2}$

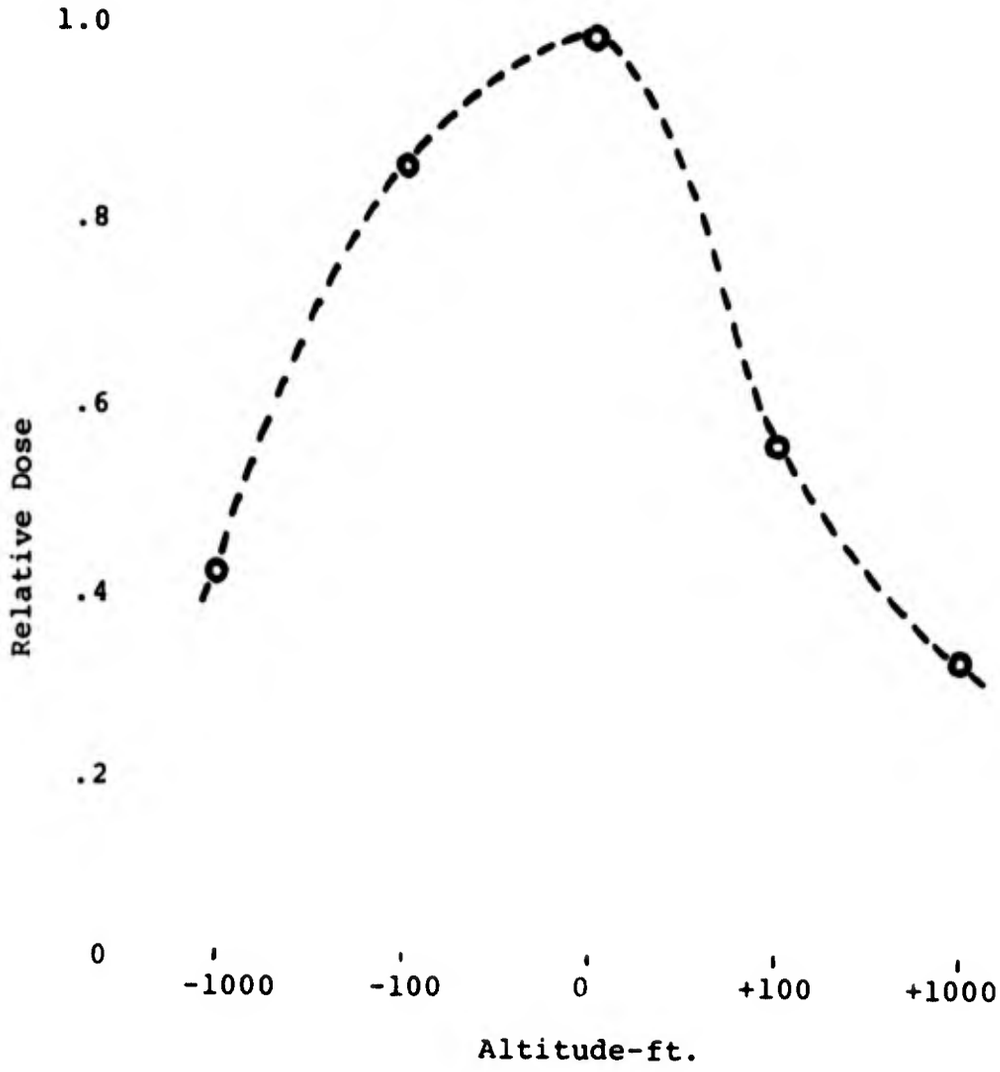

Figure 4.1 - Relative Dose vs. Terrain Altitude

The above results clearly demonstrate how non-uniform terrain may significantly affect the dose. A comparison of problems 1-5, for example, shows that the dose decreases fairly rapidly with hill height, reaching a factor of 3 reduction at 1000 feet. The dose in the valley decreases more slowly with depth, but is still down by more than a factor of 2 at 1000 feet.

4.3.1.2 Rolling Hills

Problems 6 and 7 investigated another type of terrain classified as "rolling hills". The terrain geometry did not employ contour lines, but used a series of earth cylinders set into a uniform slab of earth. Detectors were located above the elevated portion of the ground as well as in the depression between hills. A pictorial view of the geometry and summary of results is shown in Fig. 4.2. As before, the relative dose uses the flat ground result as a reference point.

It is interesting to note that the location of maximum dose in the two problems is interchanged. This deserves some comment. There are two competing effects to be considered, one of which is the increased $1/R^2$ attenuation suffered by source gammas in reaching the detector on the hill. This is due to the sloping away of the ground on either side of the detector. At the same time, however, the hilltop detector is directly exposed to a larger source area. For the 5 ft. hills, the separation between hills is large enough so that the detector in the valley already "sees" the source area of greatest importance. Thus, the $1/R^2$ effect dominates and the valley detector receives the higher dose. For the 2 ft. hills, however, the effect of extending the viewable source area is still great enough to overshadow the $1/R^2$ term, resulting in a higher dose on the hilltop.

Problem	R	H	Detector Location	Relative Dose
6	250'	5'	3' above hilltop	.64
6	250'	5'	3' above valley	.91
7	100'	2'	3' above hilltop	.84
7	100'	2'	3' above valley	.69

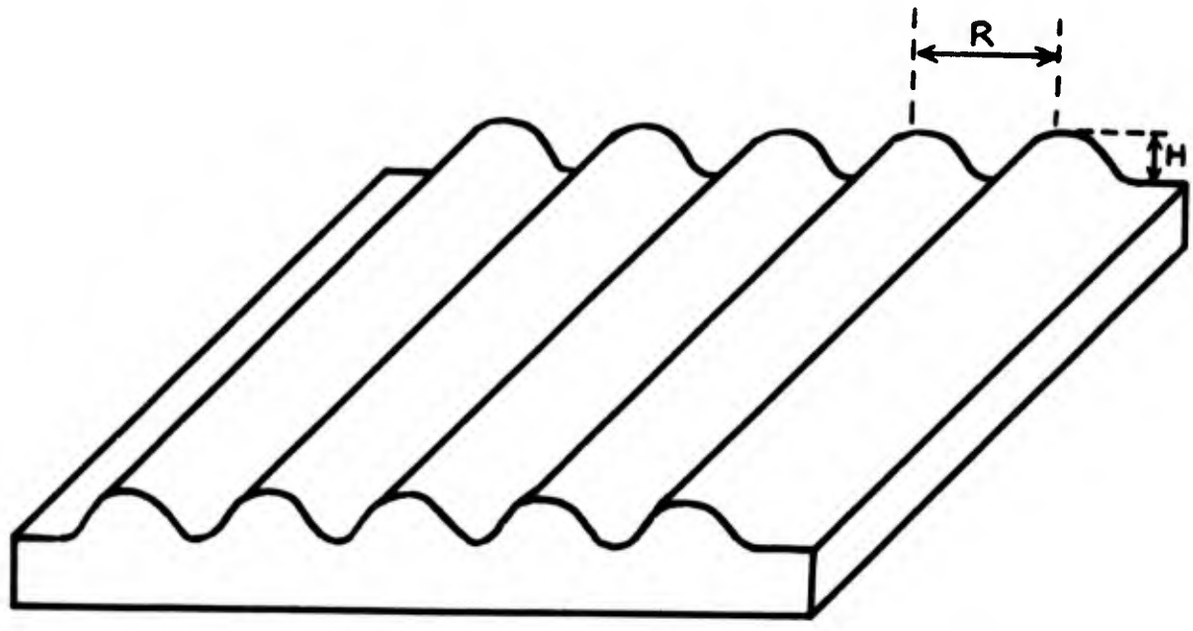

Figure 4.2 - Dose Calculations for 'Rolling Hills' Terrain

4.3.1.3 Ravines

Two additional problems were run to investigate the effects of a long, relatively narrow ravine situated on otherwise flat ground. The geometry of the problems and relative doses are given in Fig. 4.3. In problem 8 one detector point was located 3 feet above the ravine floor at its geometric center (i.e., 10 ft. from either side and 1000 ft. from either end). Problem 9 contained two detectors. One was located at the geometric center of the ravine, 3 ft. above the floor. The other, also 3 ft. above the floor, was located 1 ft. from a side wall and 1000 ft. from either end. Sources were deposited uniformly on the ground outside the ravine as well as on the floor of the ravine.

The results show the dose to be significantly higher in the wider ravine. This is to be expected since the detector in this ravine is directly exposed to five times as much source area as the detector in the 20 ft. wide ravine. In problem 9, the side location views the same area as the center location, but the average source-detector separation is greater at the side, thereby reducing the dose at the side.

Problem	W	H	L	Detector Location	Relative Dose
8	20'	10'	2000'	Center	.40
9	100'	20'	2000'	Center	.86
9	100'	20'	2000'	Side	.53

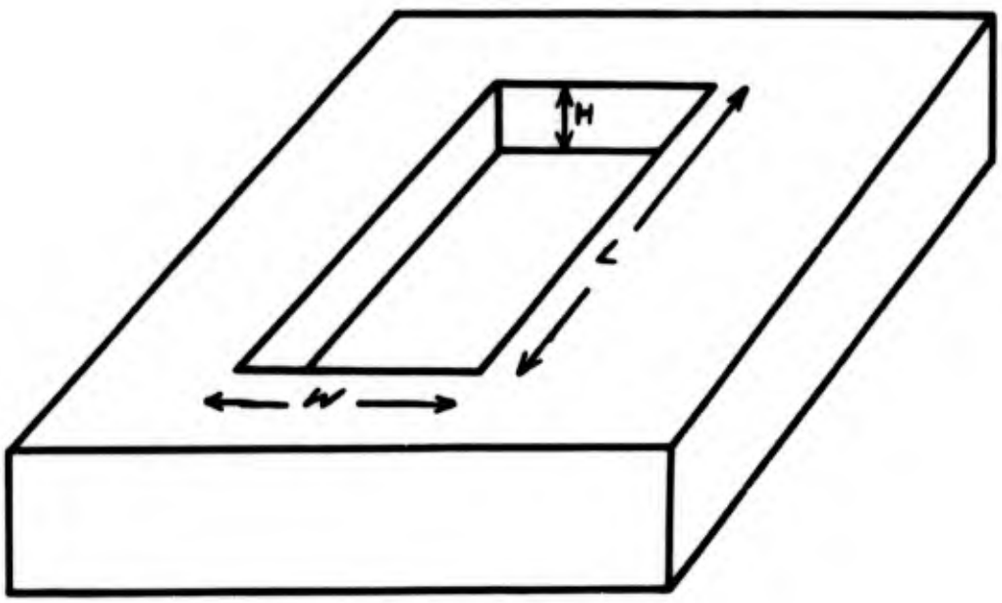

Figure 4.3 - Dose Calculations in Ravines

4.3.2 Effects of Vegetation

TERF was employed to investigate two types of vegetation, namely forests and crops. The results of these investigations are discussed separately below.

4.3.2.1 Forests

The effects of a forest on the dose near ground level involves a rather complex analysis of several phenomena, the most important of which are:

1. The average particle source height is increased by the forest. For certain types of non-uniform terrain this might actually enhance the dose near the ground.
2. The forest increases the probability of scattering in the vicinity of the detector.
3. Source gammas traversing the forest suffer greater attenuation than afforded by the same volume of air.
4. Air-scattered gammas are attenuated more before reaching the detector.

Depending on the problem, the relative importance of each of these factors can vary considerably so that the net effect of the forest is often impossible to predict in advance. Thus, a great many detailed calculations are likely to be required before any general rules on forest effects can be formulated. A number of such calculations were per-

formed as part of this study program.

The initial forest calculation was done rather early in the program, before

(a) TERF was fully developed to the point where it could handle variable fallout distributions in wooded areas. Thus, this problem was done under the assumption that all fallout was retained uniformly within the forest volume, and (b) any realistic analysis of the density and distribution of foliage in typical forests was made.

Thus, the results of this calculation (Problem 10) are not necessarily indicative of how a "typical" forest would affect the dose. In problem 10, a fairly small wooded area was located at the top of a 100 ft. hill. This hill was identical in size and shape to that used in problem 2. The forest was a square, 165 ft. on a side, containing a centrally located 20 ft. square clearing. The dose point was located at the center of the clearing, 3 ft. above the peak of the hill. The forest was represented as a homogeneous region, 40 ft. in height. The density of this region was 0.006 gm/cm^3 composed of 60% carbon and 40% hydrogen by volume. Fallout particles were deposited randomly within the forest and on the ground surface outside the forest or within the clearing.

The results of this calculation gave a relative dose at the detector of 0.56. Interestingly enough, this result is identical to that for problem 2, indicating the lack of

any effect of the forest. This is not unreasonable when one considers the four phenomena mentioned earlier. Increasing the average particle source height will bring some of the hillside source points that were formerly shielded from the detector into direct view. Thus, item 1 tends to increase the dose but this is neutralized by the increased attenuation noted in item 3. This is born out by the calculation where the uncollided dose contributions in the two problems were practically equal. Items 2 and 4 also tend to negate each other, so that the net effect of the forest was to produce no change in the dose.

The remaining forest effect problems were done with uniform terrain and made use of TERF's ability to handle fallout retention factors (i.e. percentage of fallout particles suspended in the foliage) other than 100%. Furthermore, a more realistic analysis of the density of foliage in typical tree canopies was used to obtain material compositions for these problems. The precise compositions and the mathematical formulae used to derive them are given in Appendix A.

Three forest types were investigated, each being represented by a homogeneous cylindrical region, 1000 ft. in diameter. Two of these problems were also rerun with a 100 ft. diameter clearing inserted in the middle of the forest. In each case the detector was 3 ft. above ground on the axis of the cylinder. Figure 4.4 defines the geometry, material density and fallout retention factor (R_f)

for each problem. The fraction retained was distributed uniformly with height in the trees, while the remainder settled to the ground surface. It should be mentioned that the forest region was actually a mixture of foliar material and full density air. This is justified, since the foliage in typical forests displaces only a small fraction of the total volume of air in the forest. The given material densities, therefore, include .00122 gm/cm^3 of air. Also worth noting is the fact that only the tree canopies (leaves and branches) have been represented in these problems. Neglecting the tree trunks accounts for the appearance of the forest as being "suspended" in air. As has often been shown in radiation transport calculations, a significant overestimate of γ-ray scattering results from approximating a few widely separated scatterers by a homogeneous mass containing the same amount of material. It is a better approximation to ignore these local scattering points (tree trunks) entirely.

Problem	Forest Type	Density(gm/cc)	H_t(ft)	H_c(ft)	Rf
11	Low density	.00203	20	16	35%
12	medium density	.00540	40	32	60%
13	high density	.0141	40	32	90%

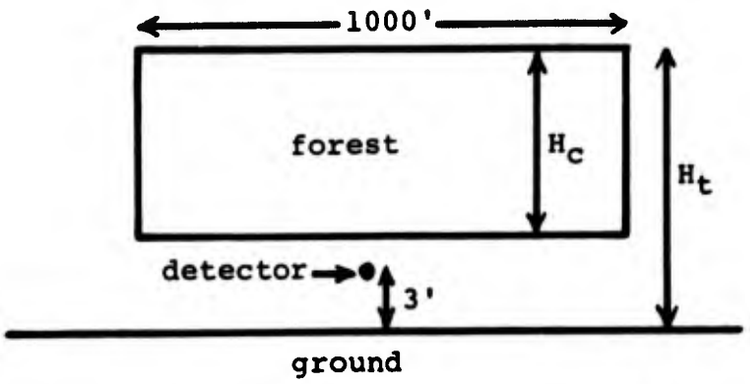

Figure 4.4 - Definition of Forest Parameters

The calculated results are shown in Figure 4.5, where relative dose is plotted against material density. Actually, these problems contained several variables including tree height, retention factor, and relative abundance of each chemical element in the forest, so that this curve does not tell the complete story. However, total density seemed to be the most meaningful independent variable for plotting the dose.

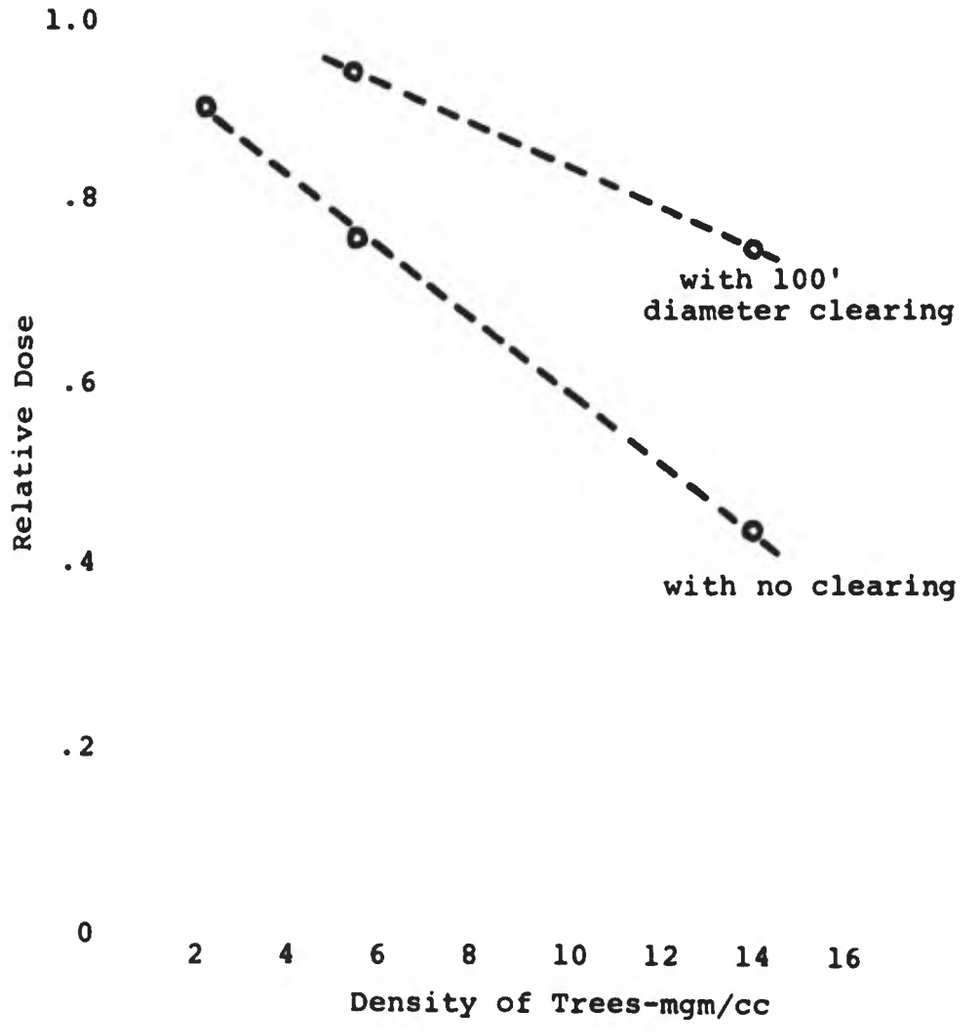

Figure 4.5 - Dose Calculations in Forests

For the problems containing no clearing, the results indicate that the dose is very nearly inversely proportional to the density. Assuming that the retention factor goes to 0 as the density approaches that of air, the lower curve should depart from this linear relationship at low densities and extrapolate to 1.0 at about 1.2 mgm/cm^3. No calculation was done for low density trees with a clearing since it was obvious from the data that this problem would give a relative dose very close to 1.0.

4.3.2.2 Crops

Two crop types were investigated on uniform terrain. The first was a 5 ft. high stand of corn containing 4 tons/acre (.00064 gm/cm^3). The second type was a 1 ft. high stand of grain, such as wheat, at 2 tons/acre (.0016 gm/cm^3). In both cases the vegetation was approximated by water and full density air was added to obtain the total density. In these problems the crop density is of the same order of magnitude as air so that the increased attenuation of γ-rays in the crops is likely to be overshadowed by geometric considerations. That is, the controlling factor is the relative positions of detector point and source particles. The retention factor is, thus, a key parameter in these problems. Knowledge of these factors in crops is quite fragmentary and is known to depend on such variables as crop maturity and weather conditions. Therefore, rather

than select a single value as typical, it was decided to run two calculations for each crop covering the extremes of retention factors. Values of 10% and 100% were selected.

Problem 14 provided the dose at two points in the corn. Detectors were located at heights within and at the top of the corn field. The results are plotted in Figure 4.6. Of main interest here is the increase in dose with increasing retention. This is the expected geometric factor, since retained particles are, on the average, in closer proximity to the detectors than those on the ground. This effect is only partially balanced by the increased attenuation in the crop material. Even for these extremes, however, the dose variation is not large, decreasing by only about 20% for a factor of 10 reduction in retention factor.

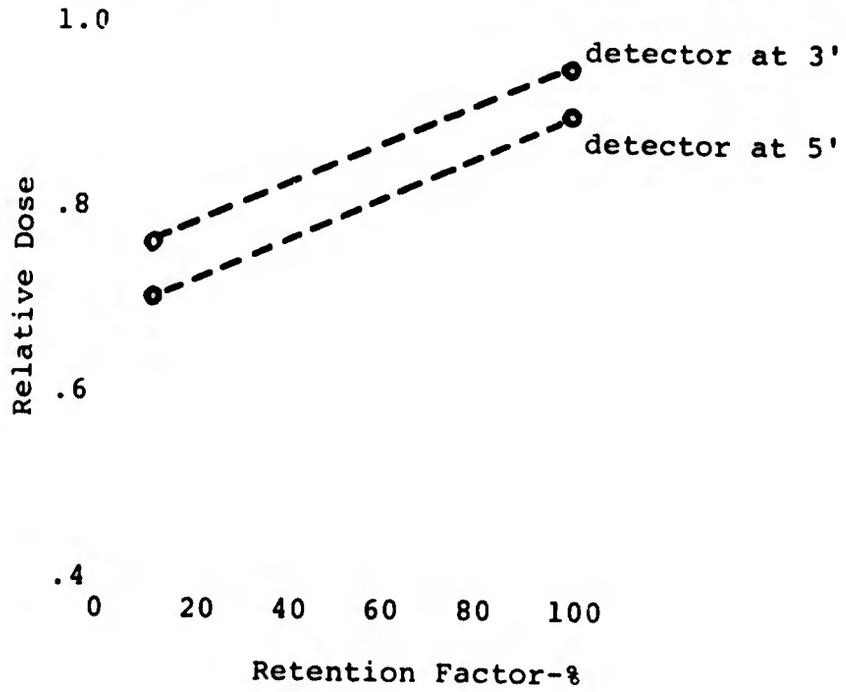

Figure 4.6 - Dose Calculations for Corn Fields

Problem 15 computed the dose in the wheat field at detector heights of 1 ft. and 3 ft. above ground. The results are given in Figure 4.7. The dose dependence on retention factor is again present but, in this case, a relative dose greater than 1.0 is obtained at the 1 ft. detector height. Even if the statistical accuracy of this answer (±6%) is taken into account the relative dose is still slightly greater than 1.0. This result is not surprising, since all source point heights are within 1 ft. of the detector height. The standard reference case, on the other hand, embodies a 3 ft. height separation. For small slant ranges (source points near the detector) this is a very substantial effect, so that a relative dose greater than 1.0 is quite reasonable.

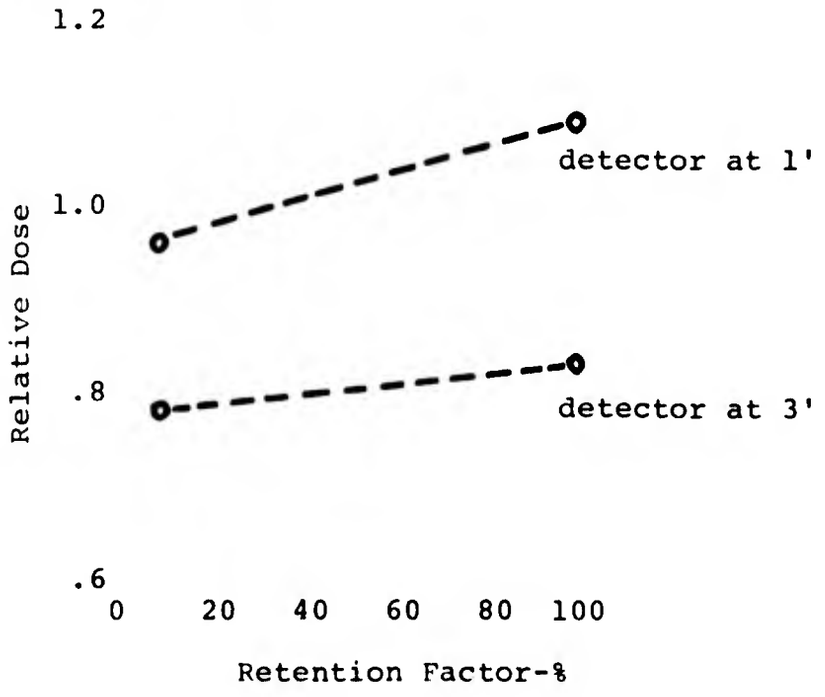

Figure 4.7 - Dose Calculations for Wheat Fields

4.3.3 Effects of Structures

4.3.3.1 Simple Houses

A set of three calculations was done to determine the dose in the basement of a small house of non-shielding construction. The house had a 9 ft. x 9 ft. floor area and an overall height of 30 ft. The basement floor was located 9 ft. below ground level with a detector point 3 ft. above the center of the floor. A thin vacuum layer was used to represent the walls and roof of the house. This affords no shielding but, being different from air, allows source particles to be deposited on the roof. Recalling the discussion of how the code deposits fallout, each particle is allowed to fall until it reaches the first non-air region. Thus, if the house had been composed of a block of air, fallout would have been deposited on the basement floor rather than on the roof. In each problem the house was situated on a different type of terrain: namely, flat ground, at the top of a 100 ft. hill, at the bottom of a 100 ft. valley. The terrain input geometries were identical to those used in problems 1,2, and 4.

Obviously, this "house" is not typical of a residential dwelling. However, these problems were conceived primarily to test the performance of TERF in calculations of this type. Problems involving more realistic structures are discussed later in this section.

The results of these three calculations are given in Table 4.3. Also included are the relative doses for the same terrain with no house (problems 1,2,4). A comparison of results shows that in all cases the presence of the house has the effect of reducing the dose by a factor of about 40. It should be noted that fallout on the roof of the house contributes .003 to the relative dose. This is independent of terrain and, therefore, represents a lower limit for the dose.

Table 4.3 - Dose Calculations for Simple Houses

Problem	Description	Relative Dose	R.D. with no house
16	house on flat ground	.028	1.00
17	house on 100' hill	.015	.56
18	house in 100' valley	.020	.86

4.3.3.2 Industrial Park

For problem 19, a typical suburban industrial park was simulated. The park consisted of ten buildings spread over an area of two acres of flat ground. The layout of the park and building dimensions are shown in Figure 4.8. The road does not actually appear in the geometry but is shown merely to orient the reader. The points labeled A and B show the locations of the two detectors in the problem. These detectors were located in the manufacturing

area of the buildings, 3 ft. above the floor. The floor of each building was at ground level.

Construction materials were typical for this type of structure. Exterior walls, consisting of 4" brick, 8" hollow block, and ½" plaster, had a mass thickness of 80 lbs/ft^2. The mass thickness of the interior block and plaster partition was 30 lbs/ft^2. The roof, represented by a homogeneous mixture of gypsum, gravel, metal beams, and ceiling tile, weighed 16 lbs/ft^2.

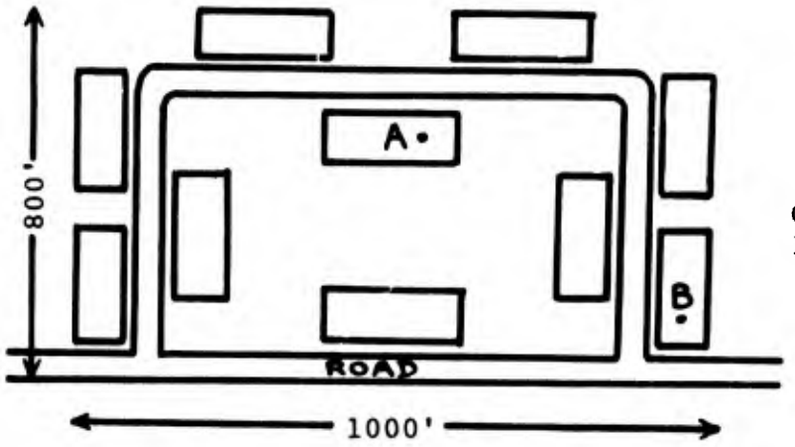

OVERALL PLAN OF INDUSTRIAL PARK

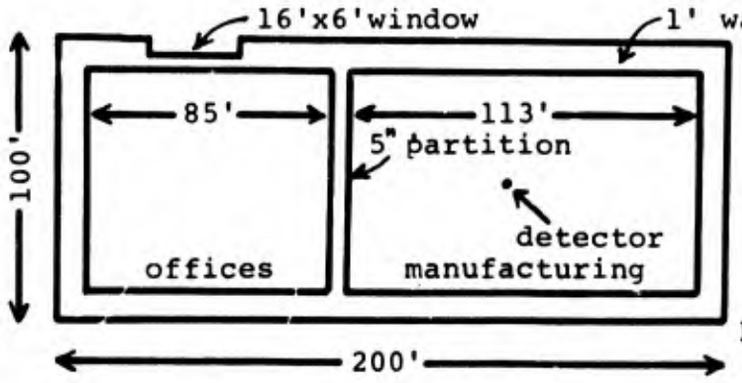

TOP VIEW OF BUILDING

building height=12.5'

Figure 4.8 - Industrial Park Geometry

The relative doses were 0.16 at point A and 0.18 at point B, indicating that about a factor of six reduction in dose is provided by these buildings. As expected, the dose at A is slightly less than at B, due to the shielding afforded by the buildings around A. Point B, being on the perimeter of the park, receives less protection.

Another point of interest is the region of the fallout field responsible for most of the dose. The problems, done in two parts, computed the contributions of "close-in" and "far-out" source areas. In the close-in problem, fallout was deposited only on the two acre area enclosing the buildings, while the far-out included everything outside this area. The close-in field was found to contribute all but a minor fraction of the dose (97% at A, 91% at B). Information of this nature is useful for establishing decontamination procedures for areas like this.

4.3.3.3 Housing Development

The final and most ambitious calculations involved the simulation of a typical suburban housing development. The development, situated on flat ground, consisted of one story, wood frame houses with basements. Figure 4.9 shows a plan view of the development, while the insert shows an enlarged view of the house in which the detector points were located. This house was modeled in some detail, including a peaked roof, interior room partitions, windows, below ground basement,

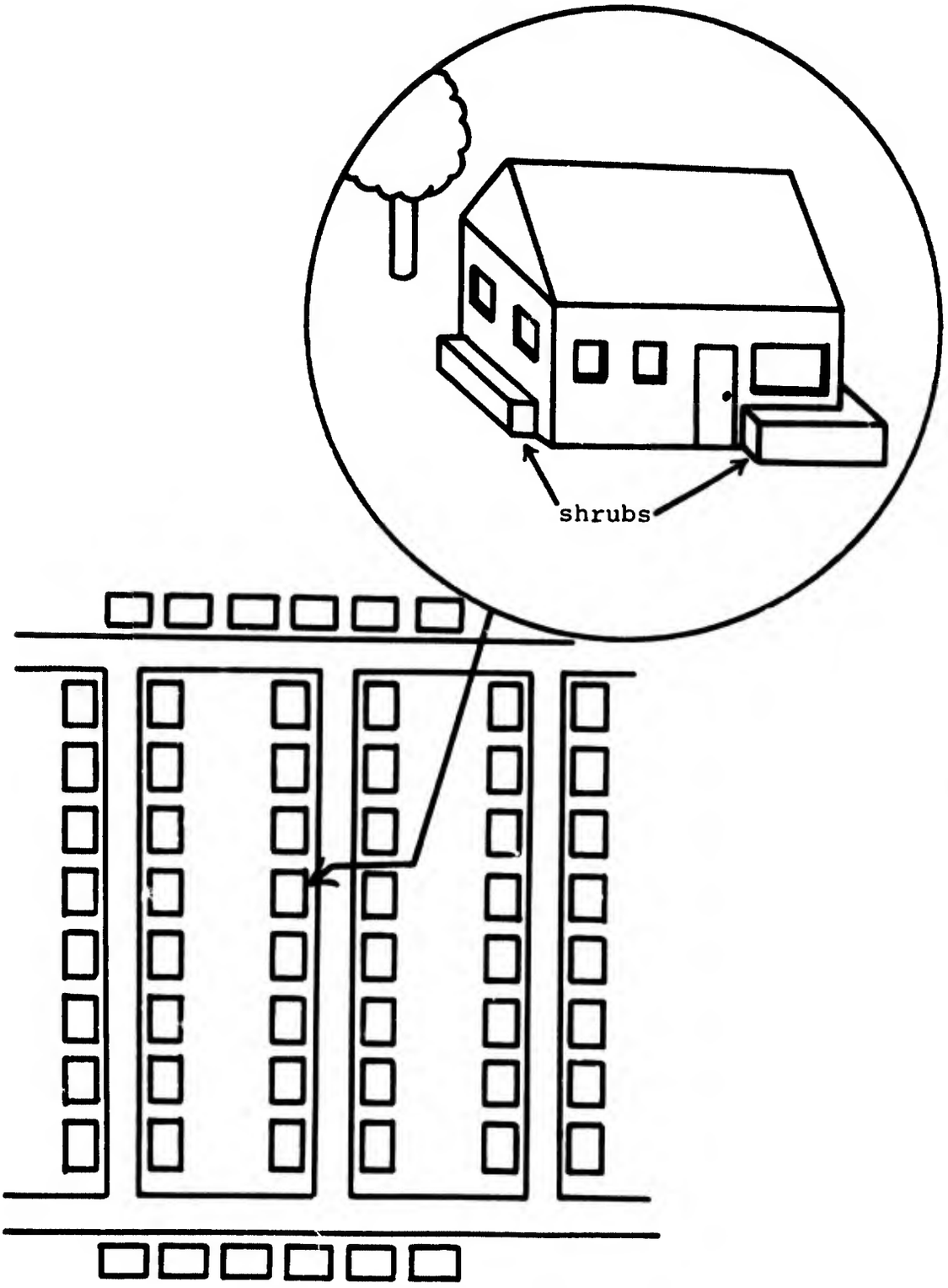

Figure 4.9 - Plan View of Housing Development Geometry

shrubbery and scattered trees in its vicinity.

Figure 4.10 shows the interior floor plan of this house. The foundation walls extended two feet above ground level, permitting the inclusion of two small basement windows. Doorways were omitted, assuming that all doors were closed. Breaks in the exterior walls indicate locations of windows, which were represented by thin slabs having the density of glass. Detector points were located as shown on the main floor and directly underneath in the basement. In both locations, detectors were 3 feet above floor level. The composition of the house, in terms of mass thickness, is given in Table 4.4.

Table 4.4 - Construction of Typical House

House Part	Mass Thickness (lbs/ft^2)
exterior walls	16
interior walls	8
foundation walls	32
roof	9
main level floor	4

The other houses in the development were modeled in less detail, with wall materials being combined to form a homogeneous low density region. Each house was, however, of the correct size, shape and mass.

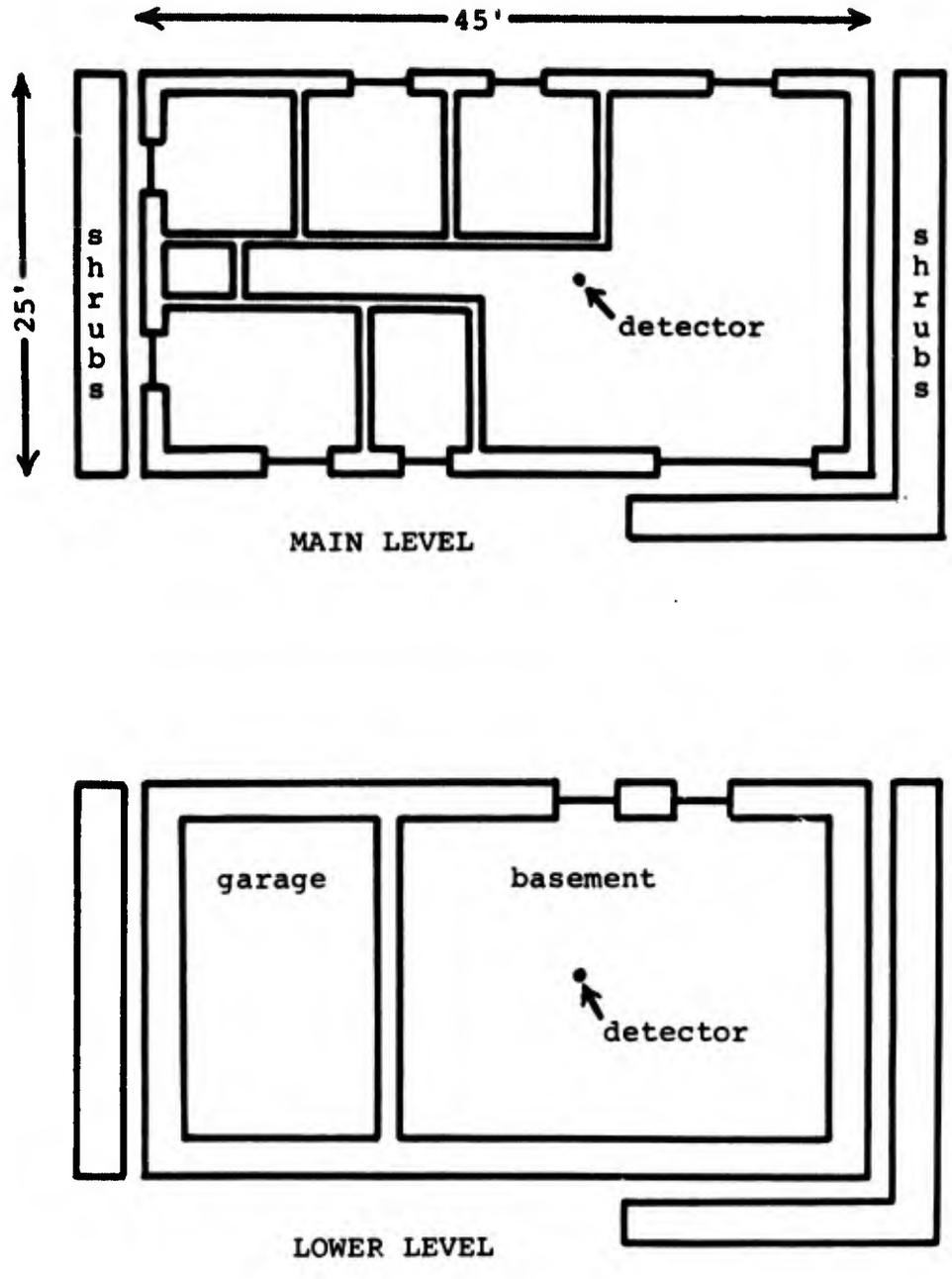

Figure 4.10 - Floor Plan of Typical House

Calculated results, in terms of relative dose, were 0.49 on the main floor and 0.17 in the basement. The contributions from fallout on the roof were computed separately in this problem and were found to provide a significant fraction of the total dose*. On the main floor about 30% of the dose comes from rooftop fallout (i.e., the roof above the detector points), while this roof contributes half the dose in the basement. This provides a strong argument for decontaminating the roofs of such houses immediately after fallout deposition. This procedure would afford more than an order of magnitude of protection in the basement as compared to the standard infinite plane case. Actually, the dose reduction would be somewhat greater than this since the roofs of neighboring houses probably contribute a not insignificant amount to the basement dose. This is especially true in this problem since there is a direct line of sight from the basement detector to the roofs of the adjacent houses. Separate calculations were not, however, done to obtain the contributions from neighboring rooftops.

To obtain a more realistic assessment of the dose in the human body, the above problem was rerun with the detector points embedded in simple man-models. These models consisted of low density water cylinders (0.8 gm/cm^3), 5'10"

*Two calculations were done. In the first, sources were deposited only on the roof of the house containing the detector points. The second calculation contained sources deposited everywhere except on the roof of this house. Total doses were obtained by summing the two results.

high and 10" in diameter. The weight of each model was, thus, 1.45 lbs. Detector points were on the axis of each cylinder, 3 ft. from the floor.

Relative doses on the main and basement levels were 0.14 and .05 respectively. This represents a reduction of about a factor of three below the corresponding detectors in air. This is reasonable since the average slant path to the axis of the cylinder is probably on the order of 15-20 cm or about one mean-free-path.

4.4 Summary of Results

For ease of comparison, all calculated results are summarized in Table 4.5.

Table 4.5 - Summary of Results

Relative Dose of 1.00 = 476000 $\frac{mR/hr}{curie/ft^2}$

Problem	Description	Detector Location	Relative Dose
1	flat ground	3' above ground	1.00
2	100' hill	3' above hilltop	.56
3	1000' hill	3' above hilltop	.33
4	100' valley	3' above trough	.86
5	1000' valley	3' above trough	.42
6	rolling hills-5' high	3' above hilltop	.64
	250' on center	3' above valley	.91
7	rolling hills-2' high	3' above hilltop	.84
	100' on center	3' above valley	.69

Table 4.5 - (continued).

Problem	Description	Detector Location	Relative Dose
8	ravine-10' deep, 20' wide	3' above floor in center	.40
9	ravine-20' deep, 100' wide	3' above floor in center	.86
		3' above floor at side	.53
10	forest on 100' hill	3' above hilltop in clearing	.56
11	low density forest	3' above ground in forest	.89
12	medium density forest	3' above ground in forest	.75
		3' above ground in clearing	.93
13	high density forest	3' above ground in forest	.43
		3' above ground in clearing	.74
14	5' high corn-10% retention	3' above ground	.76
	5' high corn-10% retention	5' above ground	.70
	5' high corn-100% retention	3' above ground	.95
	5' high corn-100% retention	5' above ground	.90

Table 4.5 - (continued).

Problem	Description	Detector Location	Relative Dose
15	1' high wheat-10% retention	1' above ground	.96
	1' high wheat-10% retention	3' above ground	.78
	1' high wheat-100% retention	1' above ground	1.09
	1' high wheat-100% retention	3' above ground	.83
16	house on flat ground	3' above basement floor	.028
17	house on 100' hill	3' above basement floor	.015
18	house in 100' valley	3' above basement floor	.020
19	industrial park	3' high in central bldg.	.16
		3' high in perimeter bld.	.18
20	housing development	3' above main floor	.49
		3' above basement floor	.17
21	housing development	3' above main floor	.14
	with man-models	3' above basement floor	.05

References

1. MAGI 6701 - A Geometric Description Technique Suitable For Computer Analysis of Both the Nuclear and Conventional Vulnerability of Armored Military Vehicles. W. Guber, et al, Mathematical Applications Group, Inc., August 1967.
2. Reactor Handbook, Vol. III Part B. Interscience Publishers, 1962.
3. "Radiation and the Patterns of Nature", Brookhaven Lecture Series No. 45, G.M. Woodwell, Brookhaven National Laboratory, March 1965.
4. The Numerical Solution of the Adjoint Transport Equation for Gamma Rays by the GADJET Code (Final report in publication). E. Friedman, et al, Radioptics Inc., March, 1968.

Appendix A

Density of Material in a Homogeneous Forest

The purpose of the following analysis is to derive an equation relating the material density in a simulated forest region to certain known parameters. This formulation is admittedly simplified but should provide at least a good first approximation to reality.

Define the density (ρ) of the tree canopy (branches and leaves) as

$$\rho = (W_C/V_C)(A_C/A_G) \qquad (1)$$

W_C = live weight of all material in the canopy (dry weight plus moisture-gms)

V_C = volume of canopy (cm^3).

A_C/A_G = projected area of canopy per unit area of ground.

Note that since we are interested only in the canopy density, the weight of the lower trunk has been ignored.

From an expression derived by Woodwell[3]

$$W_C = .6H_T D_T^2 \qquad (2)$$

where

H_T = total tree height (cm)

D_T = diameter of trunk (cm)

To compute the canopy volume (Vc) it is necessary to make an assumption as to its' shape. A conical shape, representative of the pine tree, will be assumed. Then

$$Vc = \frac{\pi}{3} R_C^2 H_C \qquad (3)$$

where

R_C = radius of base of cone (cm)

H_C = height of cone. (cm)

Substituting for V_C and W_C in equation (1) gives

$$\rho = \left(\frac{1.8}{\pi}\right) \left(\frac{H_T}{H_C}\right) \left(\frac{D_T}{R_C}\right)^2 \left(\frac{A_C}{A_G}\right). \tag{4}$$

From personal observations $H_C \approx .8H_T$, so that

$$\rho = .72 \left(\frac{D_T}{R_C}\right)^2 \left(\frac{A_C}{A_G}\right) \tag{5}$$

The ratio A_C/A_G can be evaluated from the relationships

$$A_C \equiv \pi R_C^2 \quad \text{and} \quad A_G \approx \pi \left(\frac{L}{2}\right)^2$$

where L = average distance between tree trunks (cm).

Thus, $A_C/A_G = 4\left(\frac{R_C}{L}\right)^2$.

Substitution in equation (5) gives

$$= 2.88 \left(\frac{D_T}{L}\right)^2 \text{ gms/cm}^3. \tag{6}$$

Thus, given the average diameter of a tree trunk and the average distance between trunks, the density of the canopy can be determined. This was done to obtain the composition of materials for problems 11-13.

The elemental constituents of the canopy (assumed to be mostly wood) were taken to be 60% carbon and 40% hydrogen by volume, having a molecular form $C_{1.5}H$ and a molecular

weight of 19. The number of carbon (N_C) and hydrogen (N_H) atoms per cm^3 are then

$$N_C = \frac{1.5\ N_O \rho}{19} \quad \text{and} \quad N_H = \frac{1.0 N_O \rho}{19} \quad \text{where}$$

N_O = Avegadro's number.

Using equation (6) for ρ, the results were as follows, where N_C and N_H have units of 10^{24} atoms/cm^3.

Problem	D_T(ft.)	L(ft)	$\rho(\frac{gm}{cc})$	N_C	N_H
11	0.5	30.0	.00081	.383(-4)	.256(-4)
12	1.0	30.0	.00322	1.53(-4)	1.03(-4)
13	1.0	30.0	.0129	6.14(-4)	4.10(-4)

In addition to carbon and hydrogen, full density air was added to the canopy layer, since the branches and leaves actually displace a very small fraction of the air in the forest. Thus, .00122 gm/cm^3 should be added to the above values of ρ to obtain the total densities. This is equivalent to 1.082×10^{19} atoms/cm^3 of oxygen and 4.032×10^{19} atoms/cm^3 of nitrogen.

Appendix B

Brief Description of the FRET Code

The FRET program (Fallout Radiation Energy Transport) has capabilities similar to TERF but employs a totally different approach for the solution of γ-ray transport problems. The method involves the solution of the γ-ray adjoint equation. That is, instead of selecting gammas from their initial source locations and tracking to a detector point, particles are tracked "backwards" from the detector to their ultimate source positions. From the standpoint of computing efficiency this method is more effective for problems involving widely distributed sources and a point detector. This is particularly true for detectors located within enclosed structures.

FRET evolved from the combination of the TERF and GADJET[4] programs. GADJET, conceived by Dr. M. Kalos of MAGI and recently implemented for USNRDL by Radioptics, Inc., uses the adjoint method but is limited in its ability to handle complex geometries and non-uniform terrain. Therefore, the mathematical formulation of the adjoint method, as found in GADJET, was combined with the geometry routines of TERF to form the FRET code. With the following exceptions, FRET and TERF have the same capabilities.

1. Only monoenergetic, time-independent sources are treated by FRET. This is a minor limitation since fallout problems are concerned with long-lived

isotopes where time dependence is unimportant. Assuming a single energy for the source is generally acceptable, especially for Co^{60} where 1.25 Mev is an adequate representation of the γ-ray source spectrum.

2. FRET provides the uncollided and scattered components of the total dose but does not give a detailed breakdown of the energy spectrum at the detector. Furthermore, it gives only the total dose rather than flux and dose. In most problems, however, this is irrelevant since only total dose is desired.
3. FRET handles only one detector point in a given problem. This is not a serious drawback since the total computer time consumed in running a separate problem for each detector is only slightly greater than for running all detectors in a single problem.
4. FRET allows region dependent importance sampling but does not provide for energy or angular dependent biasing. For problems involving dose from widely dispersed sources this is a minor deficiency since very low energies are unimportant and all directions may be equally important.
5. FRET provides one piece of information which is currently not available with TERF. That is, the

terrain can be subdivided either into concentric circular areas or into a rectangular grid and the dose contribution from each sub-area will be given.

Basically, then, FRET and TERF are equally capable of solving most problems. The important difference is that FRET does the same computation in less time. Initial comparisons between the two indicate that for problems of moderate complexity, FRET gives good results in about half the computing time. What is more important is the fact that the variances of the FRET answers were considerably less. For comparable accuracies, then, FRET is likely to be at least several times faster than TERF. For heavily shielded detectors this difference will be even greater, possible even a factor of ten.

At present, FRET is operational on the CDC 6600 and seems to be performing correctly. Although the program has not yet undergone exhaustive tests, there appears to be no reason to suspect its accuracy. Evidence along this line has been obtained from several calculations, performed with FRET, which can be directly compared with TERF. These comparisons are shown in Table B-1. Also given are the computer times used by the two codes. TERF running times have been normalized to one detector per problem (see Section 3.5.2) and are only approximate. The source energy in the FRET problems was 1.25 Mev.

Table B-1 - Comparisons of TERF and FRET

Problem Description	Dose (R/hr per curie/ft²) TERF	Dose (R/hr per curie/ft²) FRET	TERF / FRET	Running Time (Sec) TERF	Running Time (Sec) FRET
Industrial Park (Problem 19) Detector in Central Building	783±12%	757±6%	1.03	2000	960
Corn Field (Prob. 14) Detector 3' high 10% retained	362±3%	386±2%	.94	350	190
100% retained	454±4%	473±3%	.96	350	170
Test Problem containing a few randomly located hills	444±9%	428±3%	1.04	650	240

Unclassified
Security Classification

DOCUMENT CONTROL DATA - R & D

(Security classification of title, body of abstract and indexing annotation must be entered when the overall report is classified)

1. ORIGINATING ACTIVITY *(Corporate author)*
Mathematical Applications Group, Inc.
180 South Broadway
White Plains, New York 10605

2a. REPORT SECURITY CLASSIFICATION
Unclassified

2b. GROUP

3. REPORT TITLE
THE TERF PPOGRAM AND ITS APPLICATIONS TO THE CALCULATION OF FALLOUT RADIATION DOSE

4. DESCRIPTIVE NOTES *(Type of report and inclusive dates)*
Final Report (June, 1967 to Jan. 1969)

5. AUTHOR(S) *(First name, middle initial, last name)*
Robert A. Goldstein

6. REPORT DATE	7a. TOTAL NO. OF PAGES	7b. NO. OF REFS
January, 1969		4

8a. CONTRACT OR GRANT NO.	9a. ORIGINATOR'S REPORT NUMBER(S)
N0022867C2341	NRDL-TRC-68-56
b. PROJECT NO. OCD Work Unit 3132A	
c.	9b. OTHER REPORT NO(S) *(Any other numbers that may be assigned this report)*
d.	

10. DISTRIBUTION STATEMENT
This document has been approved for public release and sale; its distribution is unlimited.

11. SUPPLEMENTARY NOTES	12. SPONSORING MILITARY ACTIVITY
	Office of Civil Defense Office of the Secretary of the Army Washington, D.C. 20310

13. ABSTRACT

TERF is a Monte Carlo radiation transport code for computing γ-ray dose due to fallout on non-uniform terrain. The code as developed in this study incorporates extensive geometry capabilities including the unique ability to convert elevation contour line data into three-dimensional terrain representations. A variety of calculations concerned with the effects on the dose of various terrain features, structures and vegetation, are described.

DD FORM 1 NOV 65 1473 REPLACES DD FORM 1473, 1 JAN 64, WHICH IS OBSOLETE FOR ARMY USE.

Unclassified
Security Classification

14. KEY WORDS	LINK A		LINK B		LINK C	
	ROLE	WT	ROLE	WT	ROLE	WT